An Improved MLPG Method and Application in the Calculation of Electro-Thermal Field of Transmission Line

Bing Gao [1], Fan Yang [1], Minyou Chen [1], Pan Duan [2], Qing-jun Peng [3], and Yongming Yang [1]

[1] State Key Laboratory of Power Transmission Equipment & System Security and New Technology
School of Electrical Engineering, Chongqing University, Chongqing, 400044, China
gaobing.cqu@gmail.com, yangfancqu@gmail.com, mchencqu@126.com

[2] Chongqing Power Company
South Bank Bureau, Chongqing, 404100, China

[3] Postdoctoral Workstation of Yunnan Power Grid Corporation
Kunming, 650217, China

Abstract ― An improved local Petrov-Galerkin method (MLPG) is proposed to solve the general electro-thermal problems in the paper, in which the method to determine the support domain is improved. Two electro-thermal problems are analyzed and solved with the method in the paper, the results indicate that the precision of the final solution is increased. In addition, the electro-thermal field and ampacity of ±800kV ultra high voltage direct current (UHVDC) transmission line are calculated, great accuracy of the solution to the electro-thermal coupling problem is obtained. Results indicate that the maximum and minimum value of surface electric field intensity on each sub-conductor lies on the inner and outer surface, the ampacity of transmission line varies almost linearly with environment temperature inversely.

Index Terms ― Ampacity, bundled conductors, electro-thermal coupling, meshfree method, the local Petrov-Galerkin method, UHVDC.

I. INTRODUCTION

The meshfree method does not require the generation of a mesh for the solution domain, only nodes scattered in the solution domain as well as sets of nodes scattered on the boundaries. It not only overcomes the error caused by interpolation, but also in electromagnetic field, electric parameters can be derived from shape function directly. Owing to these advantages, it has received more and more attention in recent years [1-7,22].

In many fields, such as electric engineering and chemical engineering [8-11], especially for microelectronic device and electrolysis industrial materials often suffer impacts of electro-thermal coupling field. In addition, in power system, electro-thermal characteristic parameter can be an efficient method to design and dialogue [12-13].

The characteristic of device or material strongly depends on temperature which is also affected by electric parameter; in power system, a portion of device breakdown owes to overheat caused by current. Therefore, analysis of the characteristic of device under electro-thermal coupling field is particularly important.

For devices of complex physical model, if finite element method (FEM) is adopted, huge computer cost will be required for accuracy. Due to the superiority of meshfree method, in this paper, an improved MLPG method is adopted to deal with the electro-thermal coupling problems, a generalized support domain method is proposed to get higher accuracy. Then two rectangle domain problems are analyzed to verify the accuracy of this proposed MLPG method. Combing with the harsh climate of western of China, the ampacity of ultra high voltage direct current (UHVDC) transmission line is analyzed, and influence of environment temperature on ampacity is also discussed.

This paper is organized as follows, in Section II, the basic principle of MLPG is briefly

Submitted On: September 4, 2013
Accepted On: October 4, 2014

introduced. The mechanism of generalized support domain is discussed in Section III. The electro-thermal model is proposed in Section IV. In Section V, two numerical experiments are discussed firstly in order to confirm the accuracy of this improved method, then an engineering problem about the ampacity of UHVDC transmission line under extremely climate is analyzed, and Section VI concludes the study.

II. MATHEMATICAL MODEL OF MLPG

A. The MLS approximation scheme

The widely used method for construction of the meshfree shape function of MLS is adopted in this paper. Consider *u(x)* to be function of the field variable defined in the problem domain Ω. The approximation of u(x) is denoted $u^h(\mathrm{x})$:

$$u^h(\mathrm{x}) = \sum_j^m p_j(\mathrm{x}) a_j(\mathrm{x}) \equiv \mathbf{p}^{\mathrm{T}}(\mathbf{x})\mathbf{a}(\mathbf{x}), \tag{1}$$

where *m* is the number of terms of monomials, and **a(x)** is a vector of coefficients given by:

$$\mathbf{a}^{\mathrm{T}}(x) = \{a_0(x)\ a_1(x)\ \cdots\ a_m(x)\}, \tag{2}$$

which are functions of *x*.

In this paper, the square function basis is used for 2D:

$$\mathbf{p}^{\mathrm{T}}(\mathbf{x}) = [1\ x\ y\ x^2\ xy\ y^2]. \tag{3}$$

The basis assures the MLS approximation can reproduce any smooth function and its first derivative with arbitrary accuracy, the coefficient $a_j(\boldsymbol{x})$ can be obtained at the point ***x*** by minimizing a weighted discrete L_2 norm as follows:

$$J = \sum_{I=1}^n w(\mathbf{x}-\mathbf{x}_I)[\mathbf{p}^T(\mathbf{x}_I)\mathbf{a}(\mathbf{x}) - u_I]^2, \tag{4}$$

where *n* is the number of nodes in the neighborhood of ***x*** which weight function $w(\mathbf{x}-\mathbf{x}^I) \geq 0$. The u_I is the value of *u* at $\boldsymbol{x}=\boldsymbol{x}_I$. The neighborhood of ***x*** size is called the domain of influence of ***x***. By applying the difference method, the coefficient of ***a(x)*** we obtain:

$$\mathbf{a}(\mathbf{x}) = \mathbf{A}^{-1}(\mathbf{x})\mathbf{B}(\mathbf{x})\mathbf{U}_s, \tag{5}$$

where the matrices **A(x)**, **B(x)** and $\mathbf{U_s}$ are defined by:

$$\mathbf{A}(\mathbf{x}) = \sum_I^n w(\mathbf{x}-\mathbf{x}_I)\mathbf{p}^T(\mathbf{x}_I)\mathbf{p}(\mathbf{x}_I), \tag{6}$$

$$\mathbf{B}(\mathbf{x}) = [w_1(\mathbf{x}-\mathbf{x}_1)\mathbf{p}(\mathbf{x}_1),\ w_2(\mathbf{x}-\mathbf{x}_2)\mathbf{p}(\mathbf{x}_2), \ldots, w_n(\mathbf{x}-\mathbf{x}_n)\mathbf{p}(\mathbf{x}_n)], \tag{7}$$

$$\mathbf{U}_s = [U_1,\ U_2, \ldots, U_n]. \tag{8}$$

Hence, we have:

$$\begin{aligned} u^h(\mathbf{x}) &= \sum_I^n \sum_j^m p_j(\mathbf{x})(\mathbf{A}^{-1}(\mathbf{x})\mathbf{B}(\mathbf{x}))_{jI} u_I \\ &\equiv \sum_I^n N_I(\mathbf{x}) u_I, \end{aligned} \tag{9}$$

where the shape function is defined by:

$$N_I(\mathbf{x}) = \sum_j^m p_j(\mathbf{x})(\mathbf{A}^{-1}(\mathbf{x})\mathbf{B}(\mathbf{x}))_{jI}. \tag{10}$$

The following weight function is adopted in this paper [2]:

$$w(\mathbf{x}-\mathbf{x}_I) \equiv w(r) = \begin{cases} \frac{2}{3} - 4r^2 + 4r^3 & for\ r \leq \frac{1}{2} \\ \frac{4}{3} - 4r + 4r^2 - \frac{4}{3}r^3 & for\ \frac{1}{2} < r \leq 1 \\ 0 & for\ r > 1 \end{cases}, \tag{11}$$

where $r = d_I / d_{mI}$, $d_I = \|\mathbf{x}-\mathbf{x}_I\|$ and d_{mI} is the size of the domain of influence of the I^{th} node.

B. The MLPG formulation

In this section, the strong form of the steady-state heat conduction equation for two dimensional problem can be described as [8-9]:

$$\lambda \frac{\partial^2 T}{\partial x^2} + \lambda \frac{\partial^2 T}{\partial y^2} = -q_v. \tag{12}$$

The essential and the natural boundary conditions are given by the following equations, respectively:

$$T = \bar{T} \quad \text{on} \quad \Gamma_u, \tag{13a}$$

$$-\frac{\partial T}{\partial \mathbf{n}} = h(T - T_f) \quad \text{on} \quad \Gamma_q, \tag{13b}$$

where the domain is enclosed by $\partial\Omega = \Gamma_u \cup \Gamma_q$; and **n** is the outward normal direction to the boundary.

Instead of writing the global weak form for the above equilibrium equations, the MLPG methods construct the weak-form over local sub-domains such as Ω_S, which is a small region taken for each node inside the global domain. A local weak form of the governing equation (12) and the boundary conditions (13) can be written as:

$$\int_{\Omega_S}(\lambda\frac{\partial^2 T}{\partial x^2}+\lambda\frac{\partial^2 T}{\partial y^2}+q_v)w_I d\Omega$$
$$-\alpha\int_{\Gamma_{su}}(T-T_0)w_I d\Gamma=0. \quad (14)$$

Applying the divergence theorem and boundary on (14) yields:

$$\int_{\Omega_S}(\lambda\frac{\partial w_I}{\partial x}\frac{\partial T}{\partial x}+\lambda\frac{\partial w_I}{\partial y}\frac{\partial T}{\partial y}-q_v w_I)d\Omega+\int_{\Gamma_s}w_I q_n d\Gamma$$
$$=\int_{\Gamma_{sq}}-w_I h(T-T_f)d\Gamma-\alpha\int_{\Gamma su}(T-T_0)w_I d\Gamma, \quad (15)$$

where Γ_{sq} and Γ_{su} are the intersection between local sub-domain with natural boundary and essential boundary, respectively. If a sub-domain is totally inside the global domain and has no intersection between Ω_S, the $\Gamma_s=\partial\Omega_s$.

The weight function w_I used in the MLS approximation is chosen as the test function in the MLPG method. So the test function will vanish on the boundary of the local domain Ω_S and the boundary Γ_s, the equation can be rewritten as:

$$\int_{\Omega_S}(\lambda\frac{\partial w_I}{\partial x}\frac{\partial T}{\partial x}+\lambda\frac{\partial w_I}{\partial y}\frac{\partial T}{\partial y}-q_v w_I)d\Omega=$$
$$\int_{\Gamma_{sq}}-w_I h(T-T_f)d\Gamma-\alpha\int_{\Gamma su}(T-T_0)w_I. \quad (16)$$

By applying the above theory, the value of T can written as:

$$T=\sum_{i=1}^{n}N_i T_i, \quad (17)$$

where N_i represents the shape function, T is node value, and more detailed information can be seen in reference [2].

Thus, the equation (17) can be rewritten as:

$$\mathbf{KT}=\mathbf{F}, \quad (18)$$

where:

$$K_{IJ}=\int_{\Omega_s}\lambda(\frac{\partial w_I}{\partial x}\frac{\partial N_J}{\partial x}+\frac{\partial w_I}{\partial y}\frac{\partial N_J}{\partial y})d\Omega$$
$$+h\int_{\Gamma_{sq}}w_I N_J d\Gamma+a\int_{\Gamma_{su}}w_I N_J d\Gamma \quad (19)$$
$$F_I=\int_{\Gamma_{sq}}w_I h T_f d\Gamma+\int_{\Omega_s}q_v w_I d\Omega+a\int_{\Gamma_{su}}w_I\bar{T}d\Gamma.$$

III. THE PRINCIPLE OF GENERALIZED SUPPORT DOMAIN

The accuracy of MLPG method mainly relies on the shape function which is closely related to supporting domain. The common way to confirm its size is node distance multiplies by a constant, which can be described as [2]:

$$d_s=a_s d_c, \quad (20)$$

where a_s=2.0~3.0.

For regular domain, d_c is the distance between two neighborhood nodes; for irregular domain, d_c is assumed to be average distance and mainly selected by experienced equation and can be solved by:

$$d_c=\frac{\sqrt{A_s}}{\sqrt{n_{As}}-1}, \quad (21)$$

where A_s is the predefined size of supporting domain which needn't to be accurate, nA_s is the included number of nodes in A_s.

However, for inhomogeneous nodes distribution, this method may cause large error, in extremely condition (for 2D problem), when nodes in support domain all lie in x direction or y direction, the basis function can't be calculated [7].

The meshfree method can get high accuracy, if the number of nodes used for interpolation is appropriate, which mainly is about 12~28. Thus, a method to confirm the size of support domain is proposed in this paper, the size of domain can be confirmed by calculating the distance between calculated node and the other nodes. In 2D condition, the principle is as shown in Fig. 1; for particular node, searching about k nodes around it and the size of support domain is the biggest value among distances between these numbered k nodes and the calculated node multiplies a coefficient, which is 1.2~2 and k is 10~18 in this paper. As explained in Fig. 1, the total nodes in support domain and the size are labeled in color.

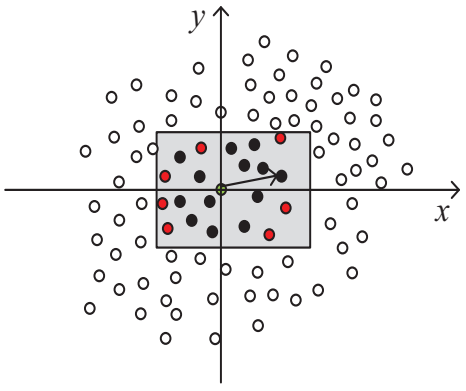

Fig. 1. The schematic diagram of the generalized support domain meshfree method.

IV. ELETRO-THERMAL FIELD MODEL

In power system, the characteristic of device is often affected by more than one field, and these fields also have interaction with each other. The typical one is electro-thermal coupling. The temperature of electric device depends on the losses which can be calculated by solving the following equation [8-9]:

$$-\nabla(\sigma(T)\nabla u) = Q_j, \tag{22}$$

where $\sigma(T)$ is the electrical conductivity, u is the electrostatic potential, Q_j is the current source.

By applying the same theory analysis just shown in the above part, equation (23) can be got:

$$\begin{aligned}&\int_{\Omega_s}(w_i\nabla(\sigma\nabla u)-w_iQ_j)d\Omega\\&=\int_{\Omega_s}w_i\left(\nabla\sigma\nabla u+\rho\nabla^2u\right)d\Omega-\int_{\Omega_s}w_iQ_j)d\Omega\\&=\int_{\Omega_s}w_i\nabla\sigma\nabla u d\Omega+\int_{\Omega_s}w_i\sigma\nabla^2u d\Omega-\int_{\Omega_s}w_iQ_j d\Omega.\end{aligned} \tag{23}$$

The second part equals with:

$$\begin{aligned}&\int_{\Omega_s}w_i\sigma\nabla^2u d\Omega\\&=\int_{\Omega_s}\nabla\left(w_i\sigma\nabla u\right)d\Omega-\int_{\Omega_s}\nabla w_i\left(\sigma\nabla u\right)d\Omega-\int_{\Omega_s}w_i\nabla\sigma\nabla u d\Omega\\&=\int_{\Gamma_i}\left(w_i\sigma\nabla u\right)\mathbf{n}d\Gamma_i-\int_{\Omega_s}\nabla w_i\left(\sigma\nabla u\right)d\Omega-\int_{\Omega_s}w_i\nabla\sigma\nabla u d\Omega.\end{aligned} \tag{24}$$

The local weak form can be written as:

$$\begin{aligned}&\int_{\Omega_s}(w_i\nabla(\sigma\nabla u)-w_iQ_j)d\Omega\\&=\int_{\Gamma_i}\left(w_i\sigma\nabla u\right)\mathbf{n}d\Gamma_i-\int_{\Omega_s}\nabla w_i\left(\sigma\nabla u\right)d\Omega-\int_{\Omega_s}w_iQ_j d\Omega.\end{aligned} \tag{25}$$

If a sub-domain is totally inside the globe domain and has no intersection between Ω_i, the first part is zero; otherwise, using the essential and natural boundary condition and trail functions whose forms are similar with equation (14), just after the same theoretical analysis in Section II, we can obtain:

$$\mathbf{Ku}=\mathbf{f}, \tag{26}$$

where

$$K_{ij}=\int_{\Omega_s}\nabla w_i(\sigma\nabla N_j)d\Omega+\alpha\int_{\Gamma_{su}}w_iN_j d\Gamma, \tag{27a}$$

and

$$f_i=\int_{\Gamma_{sq}}\sigma w_i\bar{q}d\Gamma+\alpha\int_{\Gamma_{su}}w_iu_0 d\Gamma-\int_{\Omega_s}w_iQ_j d\Omega, \tag{27b}$$

where u_0 and $\bar{q}$ are electric parameters for essential and the natural boundary.

Then the Joule heat per unit length in the conductor can be calculated as follows [8-9]:

$$q=\int\frac{JJ^*}{\sigma}dS, \tag{28}$$

where J is the current density.

The losses in a model are dependent on the temperature. The temperature distribution can be obtained by solving the nonlinear electro-thermal coupling model. Solution of this dynamic procedure can be obtained by applying the Newton-Raphson iteration method as shown in Fig. 2 [14].

In order to investigate the accuracy of the improved MLPG method, a relative error is calculated as follows [21]:

$$error=\sqrt{\frac{\sum_{i=1}^{N}(u_i^{fem}-u_i^{num})^2}{\sum_{i=1}^{N}(u_i^{fem})^2}}, \tag{29}$$

where u_i^{num} denotes the numerical solution of the i_{th} node and the u_i^{fem} denotes the FEM solution of the i_{th} node.

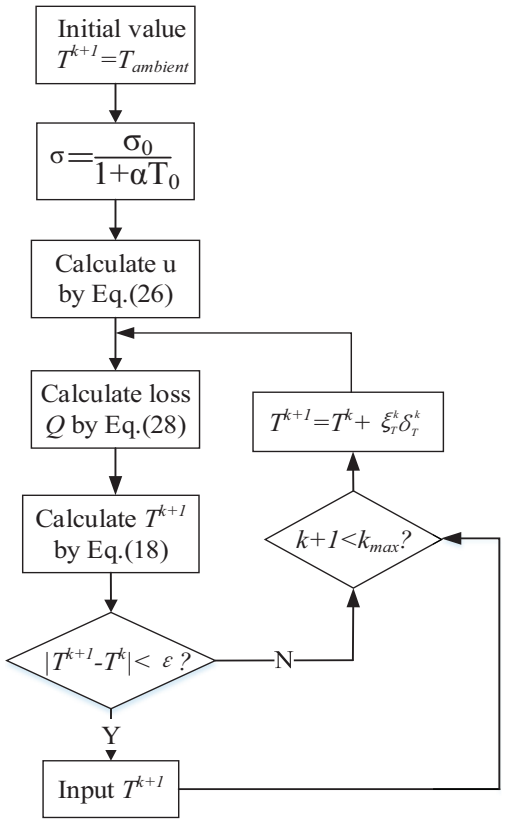

Fig. 2. The flowchart of solving the electro-thermal coupling model.

V. NUMERICAL EXPERIMENTS

In some conditions, such as the breakdown process of cable, the temperature rising is a transient process. Thus, transient electro-thermal coupling case is analyzed.

For this condition, the equation (12) can be written as [8-9]:

$$\rho c \frac{\partial T}{\partial t} = \lambda \frac{\partial^2 T}{\partial x^2} + \lambda \frac{\partial^2 T}{\partial y^2} + q_v, \tag{30}$$

where ρ is the material density; c is the specific heat capacity.

According to the derivation principle as described in Section II, the final equation is written as follows:

$$\mathbf{C}\dot{\mathbf{T}} + \mathbf{K}\mathbf{T} = \mathbf{F}, \tag{31}$$

$$\{[K] + \frac{[C]}{\Delta t}\}\{T\}_t = \{f\}_t + \frac{[C]}{\Delta t}\{T\}_{t-\Delta t}, \tag{32}$$

where $C_{ij} = \int_{\Omega_s} w(x, x_i)\rho c N_j(x) d\Omega$.

A problem domain as shown in Fig. 3 is illustrated.

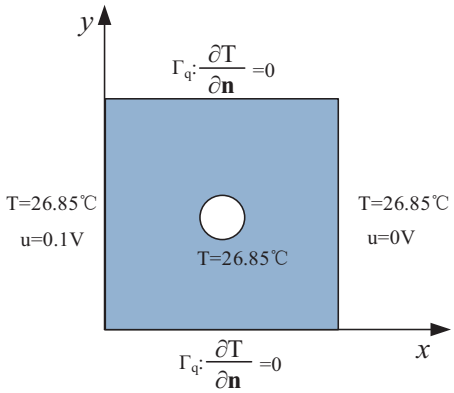

Fig. 3. The transient analysis model.

The parameter of k is set as 12, and the local quadrature domain with four subdivision cells and 4×4 integration points in each cell. The time step is set 0.05s. Both temperature distribution at t=1s and y=0.5 are analyzed, just as shown in Figs. 4 and 5.

The relative error is 0.203%, which is less than 1%, and results from Fig. 4 to Fig. 5 show very good accuracy between the improved MLPG method and FEM method; it indicates that this improved method can deal with complex problem domain well.

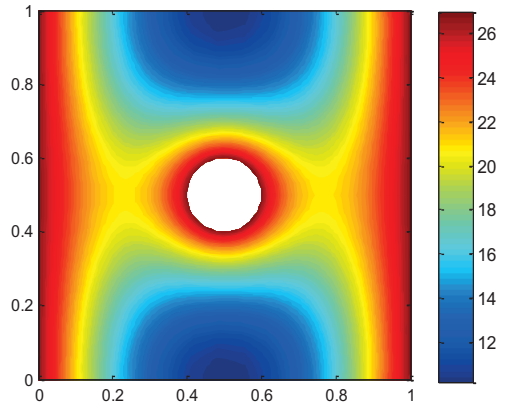

(a) Temperature distribution at t=1 of MPLG method

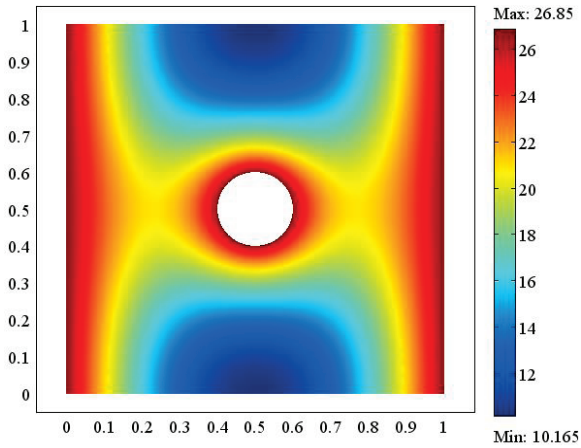

(b) Temperature distribution at t=1 of FEM method

Fig. 4. Comparisons between: (a) improved MLPG method results, and (b) FEM results.

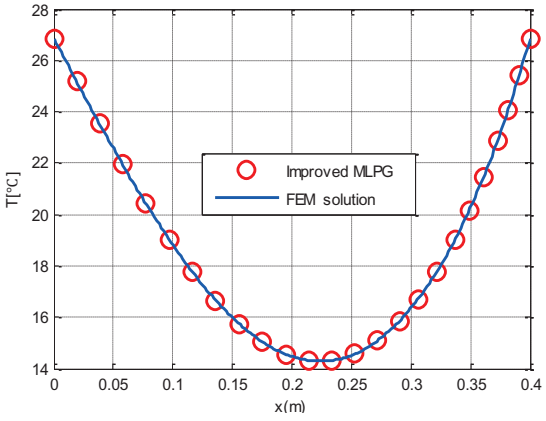

Fig. 5. Comparison between improved MLPG and FEM method along y=0.5 at t=0.5s.

In this section, a steady rectangle domain as described in Fig. 6, was first discussed.

The parameter of k is set as 12, and the local quadrature domain with four subdivision cells and 4×4 integration points in each cell. The comparison between improved MLPG method results and finite element method (FEM) results is shown in Fig. 7.

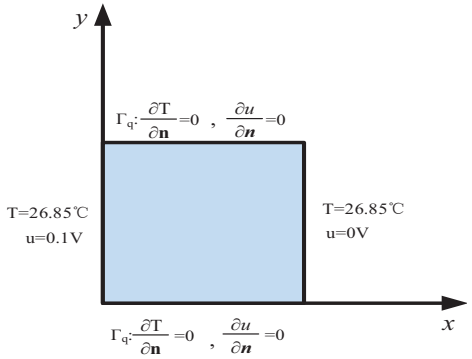

Fig. 6. The rectangle problem domain.

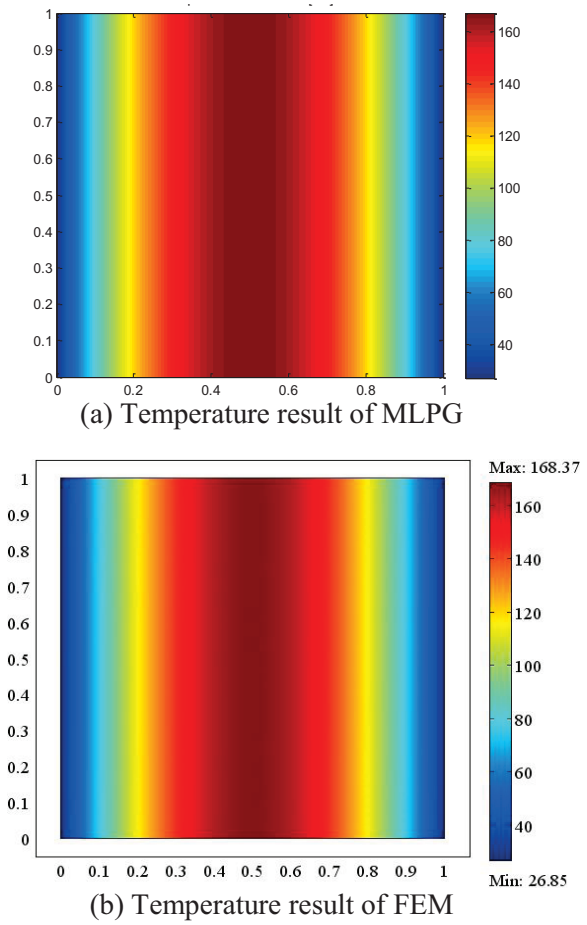

(a) Temperature result of MLPG

(b) Temperature result of FEM

Fig. 7. Comparisons between: (a) improved MLPG method results, and (b) FEM results.

The relative error between improved MLPG and FEM method is about 0.117%. We can observe good agreement between the improved MLPG results and FEM results both for electric and temperature distribution from Figs. 8 and 9. And, we can conclude that the improved MLPG method has a great accuracy. In addition, this method can be more accurate if more nodes are used in the calculation.

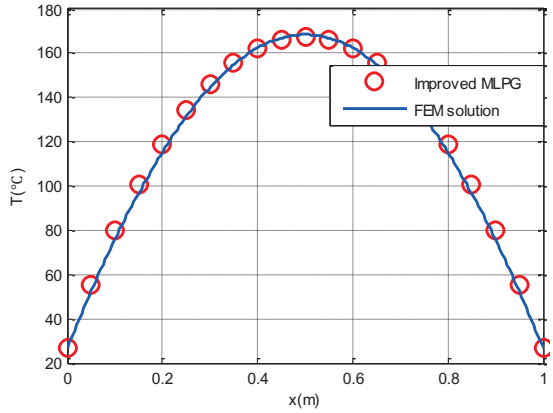

Fig. 8. Comparison between improved MLPG and FEM method along y=0.5.

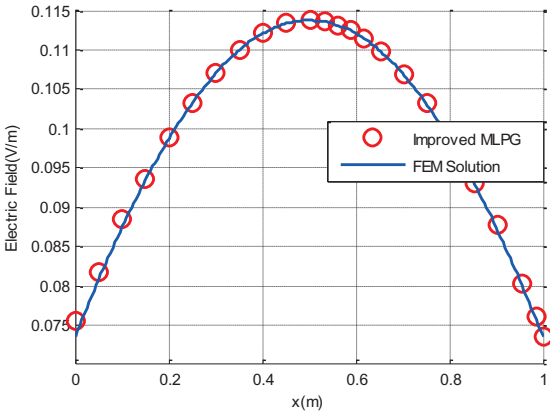

Fig. 9. Comparison along y=0.5 of the electric field.

Based on the analysis discussed in this section, a conclusion can be made that the improved MLPG method can deal with electro-thermal coupling problems well. Then, an engineering problem about the ampacity of ultra high voltage direct current (UHVDC) transmission line which will be built in the western of China where it suffers harsh climate is analyzed; then influence of environment temperature on its ampacity is also discussed.

According to the standard of China,

temperature of aluminium cable steel reinforced cannot exceed 70℃ [15-19]. However, the climate of western of China is harsh, especially for Chongqing city where the outer environment temperature can be over 40℃ in summer; in addition, with highly electrical consumption at the same time, causing serous heating. Therefore, we should make the most use of the capacity of transmission line under safety permission. Effect of wind is not taken into account because of low wind speed in this city. As the length in the axis direction is much longer than that of radial direction, in addition, the impact of sag is ignored, then the line can be regarded as limitless long. Therefore, the electro-thermal distribution can be presented by 2D situation.

As shown in Fig. 10, the main line used is 6 split conductor. Impact of sunshine is assumed as a heat flux into the domain. In order to get higher accuracy, nodes around the sub-conductors is intensive, while in other parts is coarse.

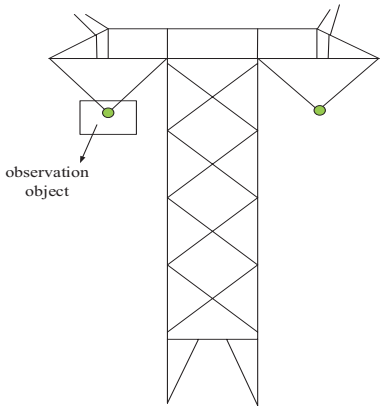

(a) Width of right way

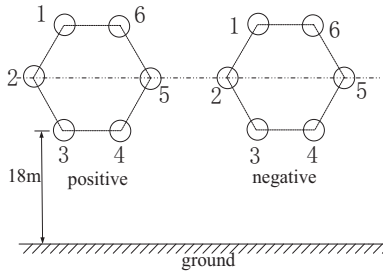

(b) Detailed explanation of observation object in (a)

Fig. 10. Schematic diagram of UHVDC transmission lines.

Because the transmission line is two-orders lower than that of the total domain, thus, an observation plane is chosen to analyze the electric and thermal characteristics. The temperature and electric field intensity distribution are shown in Fig. 11 and Fig. 12, respectively.

It can be seen that the highest temperature lies on the transmission line, because the lines are heat source. The temperature of the space surrounded by sub-conductors is higher than that of outer space, this is mainly because the inner space is nearest to all heat source. Temperature and electric field intensity distribution of the space surrounded by sub-conductors are non-uniform. Moreover, temperature in the right side of space surrounded by positive sub-conductors is higher than that of the left side. However, this situation is opposite for negative sub-conductors. This owes to the electric field intensity in space between positive pole and negative pole, which is higher than that of other space.

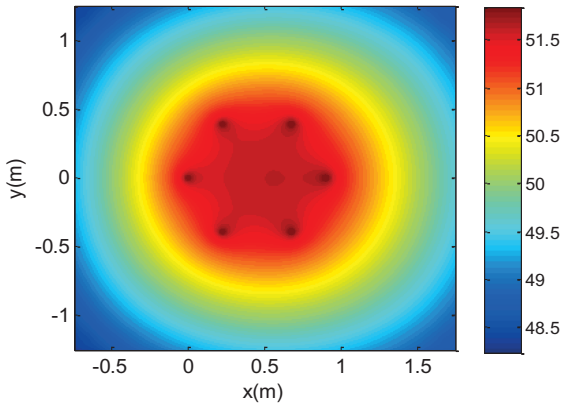

(a) The temperature distribution of space surrounded by positive sub-conductors

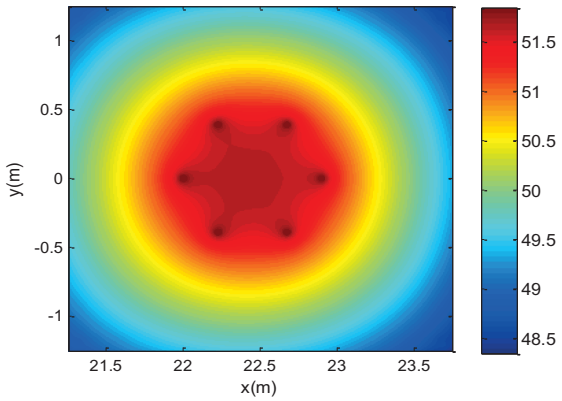

(b) The temperature distribution of space surrounded by negative sub-conductors

Fig. 11. The temperature distribution of UHDC transmission line.

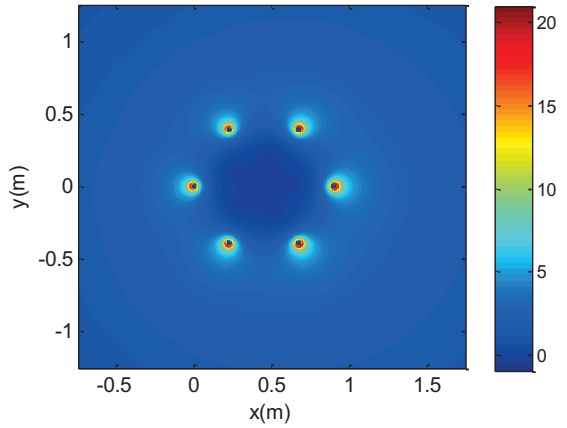

(a) The electric field intensity in space surrounded by positive sub-conductors

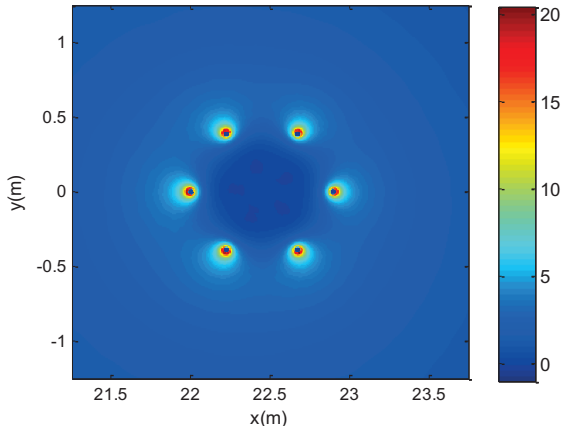

(b) The electric field intensity of space surrounded by negative sub-conductors

Fig. 12. Electric field distribution in sub-conductors.

It can be seen in Fig. 12, the electric field intensity in space between positive polar and negative polar is higher than that of other pace, the main reason is that the grounded capacitance and capacitor among sub-conductor are different due to the spacing positions and relative positions of sub-conductors [20].

At the same time, we can conclude from Fig. 12, that the maximum and minimum value of surface electric field intensity on each sub-conductor lies on the inner and outer surface, which is in the direction of the center connection line of each sub-conductor and polar conductor, respectively. And the relative location is illustrated in Fig. 13 as colored in black spots.

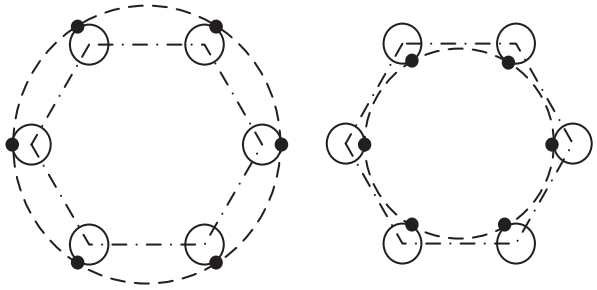

(a) Maximum electric field (b) Minimum electric field

Fig. 13. The maximum and minimum electric field intensity positions of the positive and negative sub-conductors.

Because the environment temperature has a great impact on transmission capacity, influence of it should be considered seriously for the design and operation of ultra-high-voltage transmission lines [16]. Here in this paper, the city of Chongqing is taken as an example to analyze the influence of environment temperature on the capacity of transmission line. According to the history data, the range of environment temperature of Chongqing city is 28~42℃. Variation of the ampacity with environment temperature is shown in Fig. 14.

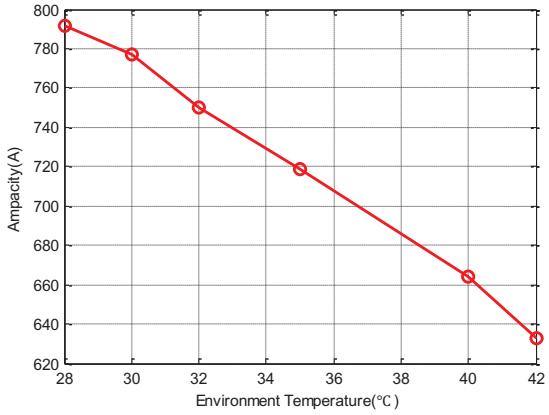

Fig. 14. The ampacity variation with environment temperature.

Results in Fig. 14 indicate that the ampacity decreases almost linearly with the increasing of environment temperature, when the temperature increases to 42℃, the ampactiy drops to 633.1A and achieves 20.02%.

VI. CONCLUSIONS

An improved MLPG method is proposed where the nodes required to construct shape function can be got directly. Then, two rectangle domain problems and ampacity of UHVDC transmission line are analyzed. The calculated results presented in this paper lead to the following conclusions:

1) The generalized support domain has a good accuracy with FEM method.
2) The improved MLPG method can deal with the electro-thermal coupling problem well.
3) Temperature of the place surrounded by of transmission lines is non-uniform; the face-to-face side is higher than the back-to-back side in the sub-conductors, the maximum and minimum value of surface electric field intensity on each sub-conductor lies on the inner and outer surface, which is in the direction of the center connection line of each sub-conductor and polar conductor
4) Ampacity of transmission line decreases almost linearly with environment temperature inversely; what's more, when the temperature increases to 42℃, the ampactiy drops to 633.1A and achieves 20.02%.

ACKNOWLEDGMENT

This work is supported by the Fundamental Research Funds for the Central Universities (No. CDJZR13150051), the Scientific Research Foundation of State Key Lab. of Power Transmission Equipment and System Security (Project No. 2007DA10512711203), and the National Natural Science Foundation of China (No. 51477013).

REFERENCES

[1] G. R. Liu, *Meshfree Methods: Moving Beyond the Finite Element Method*, Boca Raton,CRC, 2009.

[2] G. R. Liu, *An Introduction to Meshfree Methods and Their Programming*, ShanDong Univerisity Press, 2007.

[3] L. N. Williams and R. C. Mesquita, "The meshless local Petrov-Galerkin method in two-dimensional electromagnetic wave analysis," *IEEE Transactions on Antennas and Propagation*, vol. 60, no. 4, pp. 1957-1968, April 2012.

[4] M. Y. Chen, Z. Peng, and P. Hui, "Ampacity calculation for power cables using element free Galerkin method," *Proceedings of the CSEE*, vol. 30, no. 22, pp. 85-91, August 2010.

[5] P. H. Ni and S. Y. Yang, "The element free Galerkin method and its application in numerical computations of electromagnetic fields," *Electric Machines and Control*, vol. 7, no. 1, pp. 26-29, March 2003.

[6] M. L. Zhao, Y. F. Nie, and C. W. Zuo, "Local Petrov-Galerkin method for electro-magnetic field computation," *Electric Machines and Control*, vol. 9, no. 4, pp. 397-400, July 2005.

[7] Fonseca and R. Alexandre, "Improving the mixed formulation for meshless local Petrov-Galerkin method," *IEEE Transactions on Magnetics*, vol. 46, no. 8, pp. 2907-2910, August 2010.

[8] Y. C. Li, "Steady-state thermal analysis of power cable systems in ducts using streamline-upwind/Petrov-Galerkin finite element method," *IEEE Transactions on Dielectrics and Electrical Insulation*, vol. 19, no. 1, pp. 283-290, February 2012.

[9] G. Jin, "Simulation of electric field and temperature field in 30 kV DC XLPE cable," *Electric Wire & Cable*, vol. 6, no. 6, pp. 9-12, December 2009.

[10] L. Miao and R. D. Zhou, "A simulation and study of electro-thermal coupling effects in CMOSIC's," *Microelectronics*, vol. 31, no. 1, pp. 10-12, February 2001.

[11] M. Celuch, M. Soltysiak, and U. Erle, "Computer simulations of microwave heating with coupled electromagnetic, thermal, and kinetic phenomena," *Applied Computational Electromagnetics Society (ACES) Journal*, vol. 26, no. 4, pp. 275-283, April 2011.

[12] X. F. Cui, *The Multi-Physical Field Modeling and Construction Optimization of 20kA Grade Inert Electrode Aluminum Reduction Cell*, Metallurgical Science and Engineering College, Central South University, MS, Spring 2011.

[13] D. Min, L. Qi, and S. W. Wang, "Study of the coupled multidiscipline problem of electronic equipment," *Journal of Guilin University of Electronic Technology*, vol. 30, no. 4, pp. 338-342, August 2010.

[14] S. Qing, X. C. Li, and J. F. Mao, "Electrothermal coupling model based on newton-raphson iteration," *National Conference Proceedings Microwave and Millimeter Wave*, Qingdao, China, pp. 1817-1820, June 2011.

[15] L. J. Ren, G. H. Sheng, and Z. Yi, "A conductor temperature model based on dynamic line rating technology," *Automation of Electric Power Systems*, Qingdao, China, pp. 40-44, June 2009.

[16] Y. Z. Lin, "The calculation of current carrying capacity and temperature of high voltage overhead lines," *Southern Power System Technology*, vol. 6, no. 4, pp. 23-27, June 2012.

[17] G. T. Yin, *Study on Improving Transmission Line Current Capacity Based on Line Temperature Monitoring*, Department of Electrical and Eengineering, Chongqing University, MS, Spring 2011.
[18] T. O. SEPPA, "Increasing transmission capacity by real time monitoring," *Proceedings of the IEEE Power Engineering Society Winter Meeting*, New York, USA, pp. 1208-1211, August 2002.
[19] Y. Yang and D. Divan, "MLPN based parameter estimation to evaluate overhead power line dynamic thermal rating," *15th International Conference on Intelligent System Applications to Power Systems*, Curitiba, Brazil, pp. 8-12, November 2009.
[20] Z. Yu and Z. Wei, "Numerical calculation of electric field intensity on the surface of bundle conductors of overhead transmission lines," *High Voltage Engineering*, vol. 31, no. 1, pp. 23-24+27, January 2005.
[21] Q. Li, S. Shen, and S. N. Atluri, "Application of meshless local Petrov-Galerkin (MLPG) to problems with singularities, and material discontinuities, in 3-D elasticity," *Computer Modeling in Engineering & Sciences*, vol. 4, no. 5, pp. 571-585, March 2003.
[22] W. He, Z. H. Liu, and R. K. Gordon, "A comparison of the element free Galerkin method and the meshless local Petrov-Galerkin method for solving electromagnetic problems," *Applied Computational Electromagnetics Society (ACES) Journal*, vol. 27, no. 8, pp. 620-629, August 2012.

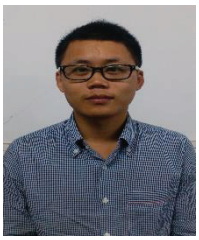

Bing Gao was born in 1987, Hunan Province, China. He received his B.E. degree in Electrical Engineering at Chongqing University in 2011. Now he is a Ph.D. candidate with the School of Electrical Engineering, Chongqing University, China. His research activities mainly include: multi-fields of power converter and meshless methods for solving electrothermal problems.

Fan Yang was born in ShanDong Province, China. He received his Ph.D. degree from the School of Electrical Engineering, Chongqing University, China and now he is a Ph.D. Supervisor in Electrical Engineering of Chongqing University. His research interests includes high voltage electrical apparatus, electromagnetic devices and sensors, electromagnetic environment of power system.

Minyou Chen was born in Chongqing, Province. He received the Ph.D. degree in Control Engineering from the University of Sheffield, Sheffield, U.K., in 1988. Now he is a Professor at the School of Electrical Engineering, Chongqing University, China. His current research interests are control, state monitoring and algorithms of new energy power system.